Water Resour Manage (2014) 28:1277–1291
DOI 10.1007/s11269-014-0540-3

A Numerical Model for Two-Dimensional Flood Routing in Complex Terrains

George Tsakiris · Vasilis Bellos

Received: 16 May 2013 / Accepted: 29 January 2014 /
Published online: 22 February 2014

Abstract In this paper, a new powerful numerical hydrodynamic in-house model is presented and tested. The model simulates flood routing in two dimensions. It is based on the solution of Shallow Water Equations using the Finite Difference Method according to the explicit McCormack numerical scheme which has shock capturing capability. The innovation of the proposed model lies in the modification of McCormack scheme by incorporating artificial viscosity through a diffusion factor in order to avoid oscillations as proposed by various researchers. Additionally, a threshold of water depth is introduced in order to distinguish the wet and dry cells of the computational domain. The model is capable of producing maps for the inundation extent, water depths and depth-averaged water velocities. Finally, the paper presents extensive testing of the model by comparison with analytical solution, experimental results and with the output of another software package in real world flood simulation studies.

Keywords Two-dimensional modelling · Shallow water equations · Flood simulation · Flood hazard maps · McCormack numerical scheme

1 Introduction

Floods are among the most disastrous natural hazards affecting millions of people around the world. Recently, the European Union set in force the Directive on Flood Risk Management presenting an innovative paradigm for the defence against floods. Among others, this Flood Directive forces the member states to identify the flood prone areas in their territory, to produce detailed flood hazard and flood risk maps, and to devise flood risk management plans for these

G. Tsakiris · V. Bellos (✉)
Laboratory of Reclamation Works and Water Resources Management, School of Rural and Surveying Engineering, National Technical University of Athens, 9 Iroon Polytechniou, 157 80 Zografou, Athens, Greece
e-mail: vmpellos@mail.ntua.gr

G. Tsakiris
e-mail: gtsakir@central.ntua.gr

G. Tsakiris
Centre for the Assessment of Natural Hazards and Proactive Planning, School of Rural and Surveying Engineering, National Technical University of Athens, 9 Iroon Polytechniou, 157 80 Zografou, Athens, Greece

vulnerable areas. As known flood hazard maps are the maps presenting the inundation area with the maximum depths and velocities encountered in each cell whereas flood risk maps are the maps presenting the projected damage losses at each cell of the computational field (European Council 2007; Tsakiris et al 2009; Parker and Priest 2012; Tsakiris 2013).

Although simple procedures can be used in the first phases of the identification and characterisation of flood prone areas, more comprehensive approaches should be used in the detailed flood risk management studies. Advanced numerical models should be used particularly in floodplains characterised by mild terrain, built and coastal environment (Bellos 2012).

Several types of numerical models for flood routing are available, some of which are available, even commercially. Generally (Néelz and Pender 2009), these models can be categorised in the following categories related to the form of the Partial Differential Equations (PDEs) which are solved: one-dimensional (1D), one-dimensional plus (1D+), two-dimensional minus (2D-) and two-dimensional (2D). The models can be also characterised by the numerical method which is used to solve the corresponding PDEs: Finite Difference Method (FDM), Finite Element Method (FEM) and Finite Volume Method (FVM).

One-dimensional models are based on some form of the 1D Shallow Water Equations (SWE) derived by integrating the Navier–Stokes equations over the cross-sectional surface of flow. The derivation of 1D-SWE (known also as Saint Venant equations) is based on assumptions which limit their use to the main direction of flow (e.g. aligned to the centre line of the watercourse). In this category, software packages such as MIKE11, HEC-RAS, FLDWAV, Infoworks-1D are the most popular. Due to limitation created by the above assumption, several extensions of the 1D approach (named 1D plus numerical models) were presented during the last two decades.

The 1D+ numerical models aim at providing more realistic simulations of flood development giving a partial of description of 2D routing. These models are also known as pseudo-2D. They are practically 1D models in which floodplains are modeled as storage cells defined only by relationships between water level and water volume. The level of water in storage cells is computed using only volume conservation, whereas no momentum conservation is incorporated. This means that water transfer from cell to cell is obtained instantaneously and very significant errors may occur in case the storage cells are large or in case the assumption of horizontality of water level is not met.

For more realistic flood inundation modeling, 2D- numerical models have been devised by solving a simplified version of the 2D-SWE. These models do not incorporate the momentum conservation principle. In this category, software packages such as LISFLOOD and JFLOW are the most popular.

In recent years, due to the capacity of computing facilities, new hydrodynamic models were devised for capturing the details of flow paths which are very complex in the real world situations, especially in flood prone areas with built environment. These models are based on the full hydrodynamic 2D-SWE and are known as 2D models. In this category, software packages such as MIKE21, CCHE2D, TELEMAC-2D, ISIS-2D, SOBEK, TUFLOW, RiverFLO-2D, Infoworks-2D are included (Néelz and Pender 2009).

It is obvious that, except from the commercial software packages, a large number of researchers have developed their in-house models adopting some of the above approaches. The in-house model presented in this paper belongs to the advanced category of full 2D models, named FLOod Wave Routing (FLOW-R2D). The model has the following features:

- it can use high resolution grids in order to capture the most important topographic peculiarities

- it can describe discontinuities of the flow (shock capturing capability)
- it resolves shallow surface water flow following complex flow paths (e.g. urban environment)
- it takes advantage of detailed GIS data for estimating the dominant model parameters all over the computational domain minimising the uncertainty embedded both in the topology and the model parameter calibration

The model offers a powerful option in detailed flood risk management studies with advanced full 2D physical representations of data and processes, whereas its efficiency is kept high. The latter feature was achieved by smart modification in the computational process resulting in very reasonable computational times for modern Personal Computers (hours).

2 Governing Equations

The FLOW-R2D model is based on 2D-SWE. These equations are derived from Navier–Stokes equations by depth integration. In conservative form, the 2D-SWE are written:

$$\frac{\partial W}{\partial t}+\frac{\partial F}{\partial x}+\frac{\partial G}{\partial y}=D \tag{1}$$

in which

$$W=\begin{vmatrix} h \\ uh \\ vh \end{vmatrix} F=\begin{vmatrix} uh \\ u^2h+0.5gh^2 \\ uvh \end{vmatrix} G=\begin{vmatrix} vh \\ uvh \\ v^2h+0.5gh^2 \end{vmatrix} D=\begin{vmatrix} 0 \\ gh\left(S_0^x-S_f^x\right) \\ gh\left(S_0^y-S_f^y\right) \end{vmatrix} \tag{2}$$

and h is the water depth, u and v are the horizontal components of water velocity along x and y direction and S_0^x, S_0^y adjust the bottom slope symbols for x and y-direction, respectively. The friction terms S_f^x and S_f^y are determined as follows:

$$S_f^x=n^2u\left(\sqrt{u^2+v^2}\right)h^{-4/3} \quad S_f^y=n^2v\left(\sqrt{u^2+v^2}\right)h^{-4/3} \tag{3}$$

where n is the Manning coefficient.

It should be mentioned that the above conservative form of the 2D-SWE has the advantage of describing the discontinuities of the flow through an appropriate numerical scheme. This claim can be proved by modifying the conservative form of 2D-SWE into weak formulation where no derivatives of water depth (h) and water velocities (u, v) appear (Vreugdenhil 1994).

3 FLOW-R2D Algorithm

The FLOW-R2D model, which is presented in this study, is based on the Finite Difference Method. The discretisation of 2D-SWE is made by the explicit McCormack numerical scheme (McCormack 1969) in a non-staggered cell-centred computational grid. We have to admit that the McCormack numerical scheme has been also used by

other researchers in modelling attempts (e.g. Fiedler and Ramirez 2000; Liang et al. 2006, 2007; Guangcai et al. 2010).

This scheme has two steps (predictor/corrector) and a second order of accuracy:

predictor step:

$$W_{i,j}^{*} = W_{i,j}^{k} - \frac{\Delta t}{\Delta x}\left(F_{i+1,j}^{k} - F_{i,j}^{k}\right) - \frac{\Delta t}{\Delta y}\left(G_{i,j+1}^{k} - G_{i,j}^{k}\right) + \Delta t D_{i,j}^{k} \tag{4}$$

corrector step:

$$W_{i,j}^{k+1} = \frac{1}{2}\left[W_{i,j}^{k} + W_{i,j}^{*} - \frac{\Delta t}{\Delta x}\left(F_{i,j}^{*} - F_{i-1,j}^{*}\right) - \frac{\Delta t}{\Delta y}\left(G_{i,j}^{*} - G_{i,j-1}^{*}\right) + \Delta t D_{i,j}^{*}\right] \tag{5}$$

where Δt, Δx, Δy are the time step and the space steps along x and y-direction, respectively.

McCormack numerical scheme is explicit and hence is stable under Courant-Friedrichs-Lewy condition (*CFL*). According to this condition, the time step Δt of each iteration is determined (Katopodes and Strelkoff 1979):

$$CFL = \left(\sqrt{u^2 + v^2} + c\right)\frac{\Delta t}{min(\Delta x, \Delta y)} \leq 1 \tag{6}$$

where c is the wave celerity.

The advantage of McCormack numerical scheme is in its shock capturing capability, which allows the description of discontinuities of the flow surface (e.g. hydraulic jumps). A disadvantage of this scheme is that it creates oscillations during the numerical simulation. In order to avoid these errors, several approaches have been proposed by various researchers (e.g. Chaudhry 2008; Fiedler and Ramirez 2000; Liang et al. 2006). In the FLOW-R2D model, artificial viscosity is added through a diffusion factor. Specifically, the first term of the corrector step becomes:

$$\omega W_{i,j}^{k} + 0.25(1-\omega)\left(W_{i+1,j}^{k} + W_{i-1,j}^{k} + W_{i,j+1}^{k} + W_{i,j-1}^{k}\right) \rightarrow W_{i,j}^{k} \tag{7}$$

where ω is the diffusion factor.

The truncation error (TE_{ω}) associated with second derivative, which adds diffusion in this modification of McCormack numerical scheme, is shown in Eq. 8. The detailed procedure determination for the calculation of TE_{ω} is presented in the Appendix.

$$TE_{\omega} = \frac{(1-\omega)}{4}\Delta x^2 \frac{\partial^2 W}{\partial x^2} + \frac{(1-\omega)}{4}\Delta y^2 \frac{\partial^2 W}{\partial y^2} \tag{8}$$

Despite of the artificial viscosity incorporated in the modification of McCormack numerical scheme which is used in this study, the scheme still has second order of accuracy (TE_{ω} is proportional to Δx^2 and Δy^2). It is suggested that ω should take values between 0.9 and 1.0.

Another difficulty of the numerical process is the moving boundaries between wet and dry bed. Generally, the 2D-SWE governing equations hold only where water exists. But in most cases, either there are no data for the basic flow of the river or the initial conditions represent a completely dry domain (e.g. urban environment). Especially in Southern Europe, rivers and

streams are of intermittent flow or their basic flow is rather insignificant in comparison with a possible flood flow.

These conditions led various researchers to produce algorithms which avoid this difficulty of the dry bed. Some researchers set a small value of water depth in the entire computational field as an initial condition (Fiedler and Ramirez 2000). In the proposed model, a threshold of water depth which distinguishes wet and dry cells is added (h_{dry}). If water depth is determined below of this threshold during the calculations, flow velocity is taken equal to zero. This method has been also used by Liang et al. (2006) and has the advantage that can also describe the exponential increase of bottom friction in small water depths. Needless to say that threshold value determination is of importance and depends on grid cell size. The threshold should not take high values in order to simulate very shallow flows such as flows in urban environments (Hunter et al. 2008), and not very low values which may create instabilities during the implementation of the model.

In regard to the boundary conditions, it should be mentioned that several options are incorporated in the model. For the upstream boundary conditions, a hydrograph or a constant discharge (Dirichlet) can be used with the assistance of a discharge-elevation rating curve of the upstream cross-section. There is also an option for solid wall boundaries with reflection (vertical flow velocity in the wall is inserted in SWE with opposite sign).

For the downstream boundary conditions, several options are also available. These include a hydrograph, a given water stage for the sea or a lake, or the Neumann boundary condition; the latter condition implies that the downstream boundary condition is determined by the hydraulic characteristics of the upstream space step. Last alternative condition is the kinematic wave condition (open boundaries) in which the water depth is determined fulfilling the following equation:

$$\frac{\partial h}{\partial t} + c\frac{\partial h}{\partial x} = 0 \tag{9}$$

Lateral boundary conditions can be determined either by solid walls or can be open. Besides, there are cases in which it is not necessary to determine the boundary conditions if the topography of the computational field allows water to determine its boundaries on its own.

Finally, the options for initial conditions incorporated in the model are: dry bed in the entire computational field or water depth in an area either in a moving condition (e.g. basic flow) or in a static condition (e.g. dam-break problem).

4 Numerical Verification of the Model

The first numerical experiment with FLOW-R2D model is a numerical simulation of the flow transition from supercritical to subcritical conditions. Moreover, a comparison with the analytical solution was performed. With this numerical experiment, FLOW-R2D model is tested for uniform and steady conditions. Additionally, the shock capturing capability of the McCormack numerical scheme is also tested for the hydraulic discontinuity of the expected hydraulic jump.

Specifically, the above experiment consists of a prismatic orthogonal channel with length L=100 m where the bottom slope in the upstream half length section is 3 % (steep slope/supercritical conditions) and the rest 0.03 % (mild slope/subcritical conditions). The cross-

section of the channel is 20 m wide (B=20 m), the Manning coefficient is n=0.030 s/m$^{1/3}$ and constant inflow is Q=10 m^3/s.

According to the Manning equation for infinite channel width and uniform steady flow, the normal depth for the upstream section is h_n=0.23 m and for the downstream h_n=0.92 m:

$$q = \frac{1}{n} h_n^{5/3} S_o^{1/2} \tag{10}$$

where q is the unit discharge equal to Q/B.

It should be mentioned that the Manning equation for infinite channel is preferred since the influence of the lateral boundaries in flow characteristics is negligible. The critical depth for the above inflow is calculated by the following equation equal for 0.29 m:

$$h_c = \left(\frac{q^2}{g}\right)^{1/3} \tag{11}$$

Needless to say that in the first and the last section of the channel, the flow can be assumed to be uniform and steady and a hydraulic jump will be formed during the transition from supercritical to subcritical conditions. According to this, three possible water profiles may occur at the transition: a) hydraulic jump occurs at the steep section and therefore an S1 profile of Gradually Varied Flow (GVF) is produced until the water depth reaches the normal depth of the subcritical condition b) hydraulic jump occurs at the mild section and therefore an M3 profile of GVF is produced until the water depth reaches the normal depth of the subcritical condition c) normal depths are conjugate and therefore the hydraulic jump occurs just in the change of the bottom slope.

According to the analytical process of this hypothetical scenario, the hydraulic jump occurs at the steep section and therefore an S1 profile of GVF is produced until the water depth reaches the normal depth of the subcritical condition. Conjugate depths are determined by the conservation of the Specific Force:

$$\frac{h_2}{h_1} = \frac{1}{2}\left(\sqrt{1 + 8Fr_1^2} - 1\right) \tag{12}$$

where Fr_1 is Froude number calculated with h_1.

The length of hydraulic jump is determined by the following experimental equation for h/B <0.1 (Chaudhry 2008):

$$\frac{L_r}{h} = 160 tanh\left(\frac{Fr}{20}\right) - 1.2 \tag{13}$$

where L_r is the length of the hydraulic jump.

The water depths in the GVF section are determined by the Energy Conservation equation as follows:

$$\frac{dh}{dx} = \frac{S_0 - S_f}{1 - Fr^2} \tag{14}$$

where dh/dx is the water depth derivative with respect to length.

For the numerical simulation with FLOW-R2D model, at the upstream section of the channel, the flow is supercritical, so three hydraulic variables should be determined for the upstream boundary conditions. At the downstream section of the channel, the flow is

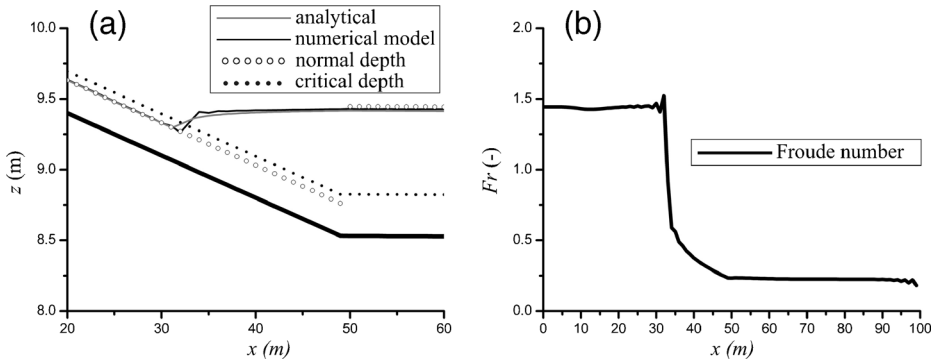

Fig. 1 **a** Water depth profile concentrated at the transition section at the streamwise central axis of the channel **b** Froude number values profile at the streamwise central axis of the channel

subcritical and therefore one hydraulic variable should be determined for the downstream boundary conditions (Abbott 1979). It should also be mentioned that for the numerical modelling, the space step is 1 m in both directions, the dry bed threshold $h_{dry}=3\times10^{-3}$ m, the Courant number is assumed $CFL=0.1$ and the diffusion factor $\omega=0.99$ for this application. It is interesting to see that the performed simulation used the Time-Marching Method in which the initial conditions consist of a dry bed and the flow reaches its permanent characteristics after a considerable time has elapsed.

In the Fig. 1a, the comparison between numerical and analytical results in the permanent state is shown. Specifically, the water depth profile is illustrated at the streamwise central axis of the channel. This snapshot is focused on the transition section of the channel. It is concluded that a high degree of convergence is achieved between numerical and analytical results. Besides, the hydraulic jump according to the analytical solution occurs at $x=32.3$ m when according to numerical solution occurs at $x=32.9$ m. The position of the hydraulic jump of the numerical solution can be determined from the Froude number values. The Froude number profile at the streamwise central axis of the channel is presented in the Fig. 1b.

The next numerical experiment is a quality control for a hypothetical scenario which tests the symmetric shock capturing capability and the availability of the reflection boundaries of a solid wall. More specifically, a circular dam-break in dry bed is examined with a water depth

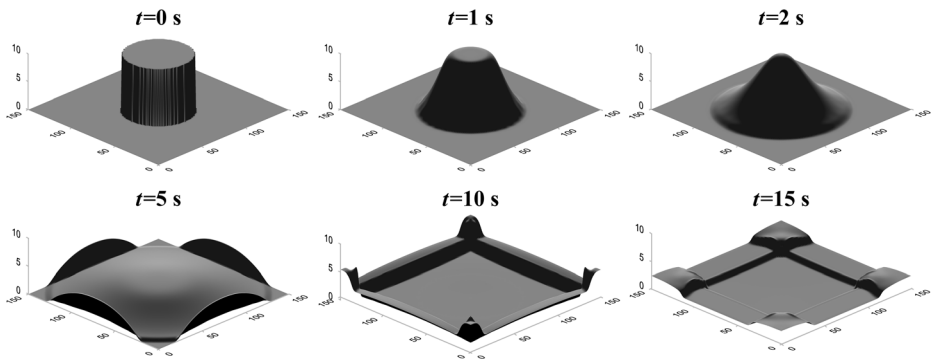

Fig. 2 The development of circular dam-break at various time horizons

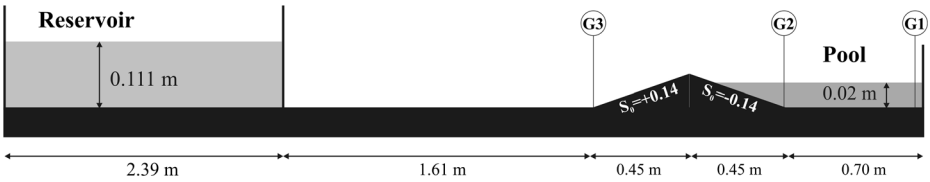

Fig. 3 The experimental set-up

of 10 m and a radius of 30 m. The reflection boundaries of solid walls at the boundaries of the computational field are examined simultaneously. The Manning coefficient is assumed n= 0.012 s/m$^{1/3}$ for the entire computational field. This test has been used in the past by various researchers in order to validate their models (e.g. Anastasiou and Chan 1997; Gwo-Fong et al. 2003; Erpicum et al. 2010). The results of the model are shown in Fig. 2.

In this application, the model was run with space step 1 m for both directions, dry bed threshold $h_{dry}=7\times10^{-5}$ m, Courant number CFL=0.1 and diffusion factor ω=0.9.

5 Experimental Validation of the Proposed Model

Apart from the numerical examples which were presented previously, it is appropriate to validate the model with real experimental data. Several researchers have developed experimental set-ups simulating various flow scenaria (e.g. Testa et al. 2007; Emelen et al. 2012). In this paper, an experiment which was conducted by Soares-Frazao (2007) and simulates a dam-break case is used in order to validate the proposed model (Fig. 3). This specific experimental set-up is also used by some other researchers in order to validate their models (Erpicum et al. 2010). The width of the experimental channel is 0.5 m. The vertical diaphragm is used to simulate the abrupt flow from the dam. The experimental data include the water-profile in various time moments and water depth time series for upstream from the triangular bottom sill, downstream from this sill and at the end of the channel (Fig. 3: G3, G2, G1 respectively).

The comparison between numerical results produced by the model and the experimental results is shown graphically in Fig. 4. Further illustration is provided for comparison purposes for the three points G3, G2 and G1 at which experimental results are available (Fig. 5). It

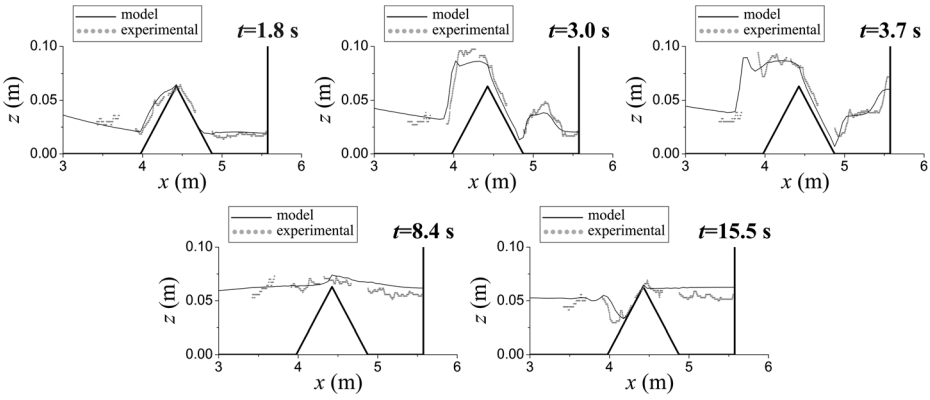

Fig. 4 Water profiles at various time horizons

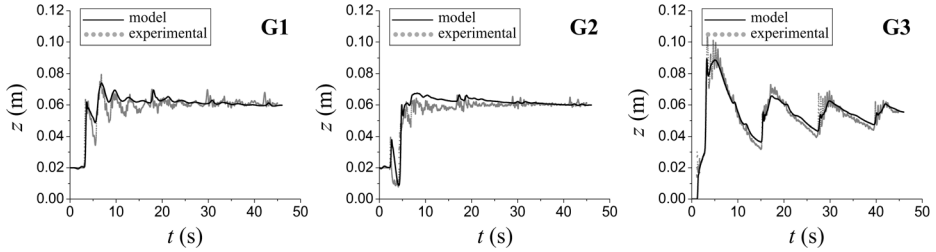

Fig. 5 Water depth with respect to time at G1, G2 and G3 points

should be mentioned that in this application, the dry bed threshold was set $h_{dry}=3\times10^{-6}$ m, Courant number $CFL=0.1$ and diffusion factor $\omega=0.99$. The Manning coefficient is estimated $n=0.011$ s/m$^{1/3}$. Space step in streamwise direction is $\Delta x=0.05$ m and in transversal direction is $\Delta y=0.01$ m.

Apart from the graphical comparison, the goodness of fit between numerical results produced by the model and experimental results is also calculated through three well-known performance indicators, namely the Pearson Correlation Coefficient (*PCC*), the Nash-Sutcliffe Coefficient of Efficiency (*NSE*) and the Index of Agreement (*IA*). The *PCC* indicator (Pearson 1895) has range from 0 to 1 and is calculated by the Eq. 15:

$$PCC=\frac{n\sum_{i=1}^{n}\left(h_{num}h_{exp}\right)-\sum_{i=1}^{n}\left(h_{exp}\right)\sum_{i=1}^{n}\left(h_{num}\right)}{\left[n\sum_{i=1}^{n}\left(h_{exp}\right)^2-\left(\sum_{i=1}^{n}\left(h_{exp}\right)\right)^2\right]\left[n\sum_{i=1}^{n}\left(h_{num}\right)^2-\left(\sum_{i=1}^{n}\left(h_{num}\right)\right)^2\right]} \quad (15)$$

where h_{exp} is the experimental water-depth data and h_{num} is the water depth data derived from the numerical simulations performed by the model under assessment.

The *NSE* (Nash and Sutcliffe 1970) ranges from $-\infty$ to 1 (Eq. 16):

$$NSE=1-\frac{\sum_{i=1}^{n}\left(h_{num}-h_{exp}\right)^2}{\sum_{i=1}^{n}\left(h_{exp}-\overline{h}_{exp}\right)^2} \quad (16)$$

Finally, the *IA* indicator with values from 0 to 1 is calculated by Eq. 17 (Willmott 1981):

$$IA=1-\frac{\sum_{i=1}^{n}\left(h_{exp}-h_{num}\right)^2}{\sum_{i=1}^{n}\left(\left|h_{num}-\overline{h}_{exp}\right|+\left|h_{exp}-\overline{h}_{exp}\right|\right)^2} \quad (17)$$

In Table 1, the values of the performance indicators for assessing the performance of the proposed model, are presented. The assessment was performed for the five water profiles (at different time horizons) and for the three time series (G1, G2, G3). The high values of indicators achieved, show that there is a high degree of convergence between the experimental

Table 1 Performance indicators for the comparison between the experimental and the numerical results

t (s)	1.8	3.0	3.7	8.4	15.5	G1	G2	G3
PCC	0.96	0.96	0.95	0.63	0.83	0.95	0.94	0.98
NSE	0.91	0.91	0.89	−0.19	0.21	0.89	0.86	0.95
IA	0.97	0.97	0.97	0.65	0.81	0.97	0.96	0.99

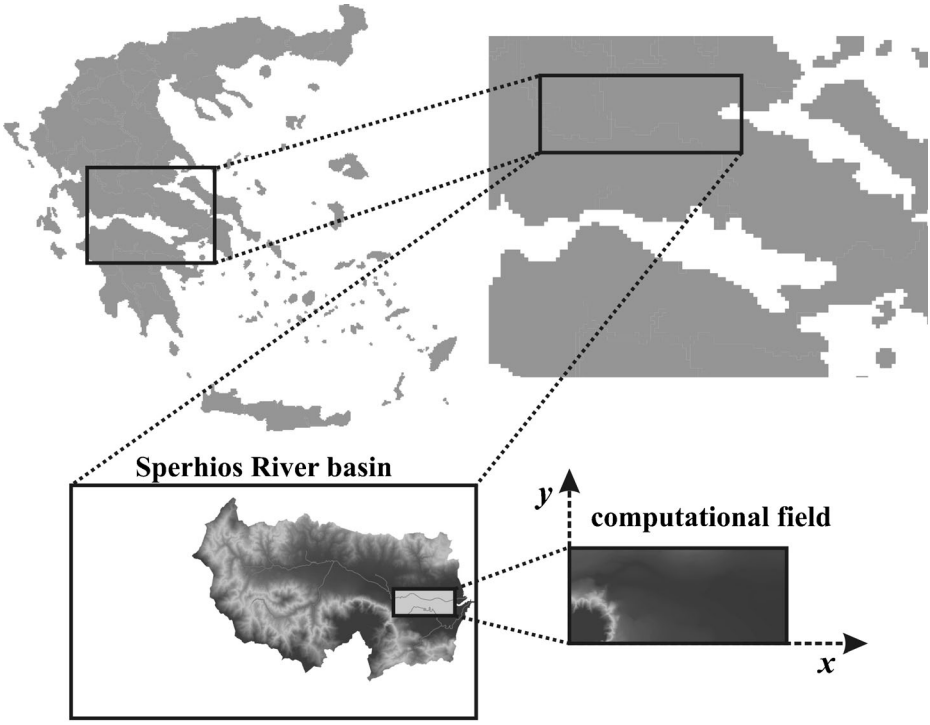

Fig. 6 Map of Sperhios River basin

and the numerical results produced by the model. The explanation of lower values of the performance indicators in times *8.4 s* and *15.5 s* may be partially attributed to the bouncing effect in which no direct estimation of energy loss is accounted for.

6 Case Study: The Proposed Model Versus CCHE2D

An additional test for FLOW-R2D model is to be compared with a well-known software package which has been tested and used extensively in the past. In this paper, the CCHE2D

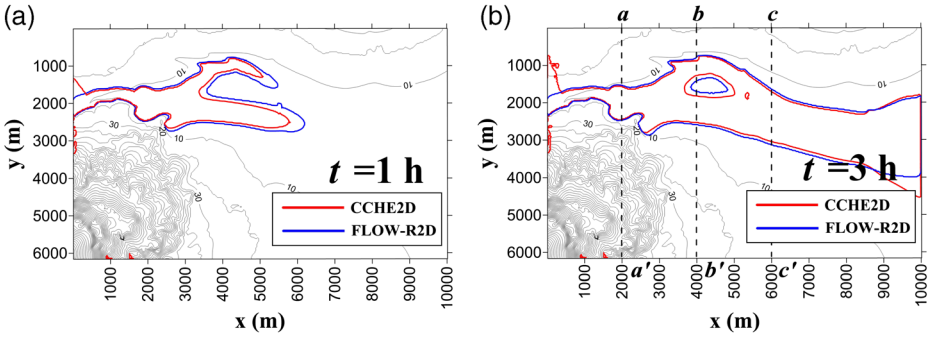

Fig. 7 **a** Inundation area with CCHE2D and FLOW-R2D model for T=50 years, at t=1 h **b** Inundation area with CCHE2D and FLOW-R2D model for T=50 years, at t=3 h

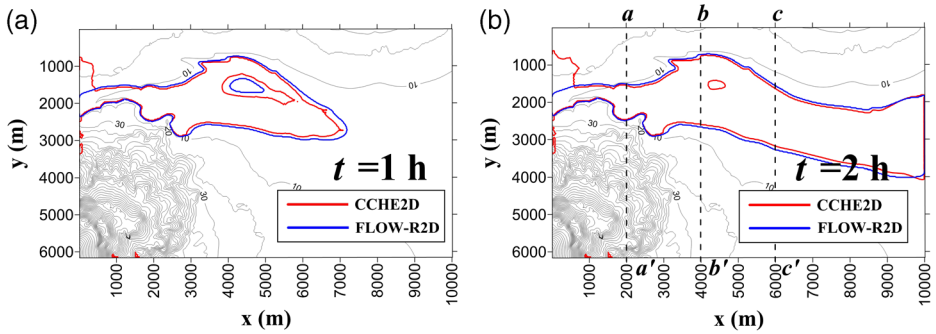

Fig. 8 **a** Inundation area with CCHE2D and FLOW-R2D model for T=500 years, at t=1 h **b** Inundation area with CCHE2D and FLOW-R2D model for T=500 years, at t=2 h

software (based on the Finite Element Method and a depth-integrated form of Navier–Stokes equations) of the U.S. "National Center for Computational Hydroscience and Engineering" (Jia and Wang 1999) has been chosen in order to compare FLOW-R2D model in a set-up of the real world (Fig. 6). The area selected is the downstream section of Sperhios River at the region of Central Greece, is of particular mild terrain and therefore transverse flow velocity is of the same magnitude with the respective streamwise velocity component. Additionally, the width of the main channel is quite small with respect to the grid size adopted and therefore there are no detailed topographic data representing the river banks of the main channel. This fact leads to the conclusion that the whole area should be approached as the entire floodplain area and therefore a 2D flood routing modelling approach is more appropriate. Instead the 1D modelling is appropriate only for the main channel flow.

In Figs. 7, 8, 9, and 10, the comparison between the results of FLOW-R2D model and CCHE2D model, for two Return Period (T) scenarios (T=50 and 500 years) for the inundation area and various cross-sections at specified time moments, is presented. In the first scenario, just the peak discharge of flood hydrograph Q=2,200 m^3/s (T= 50 years) is assumed as upstream boundary condition (constant inflow). The same applies to the second scenario Q=4,000 m^3/s (T=500 years) (Koutsoyiannis et al. 2003). The Manning coefficient was estimated n=0.03 $s/m^{1/3}$ for the entire computational field. It should be mentioned that the constant inflow, as upstream boundary condition, results in flow characteristics which become permanent in the whole computational domain after a certain simulation time It can be seem that this stabilization (Figs. 7b and 8b for the first and second scenario, respectively) appears in the first scenario with the lower inflow.

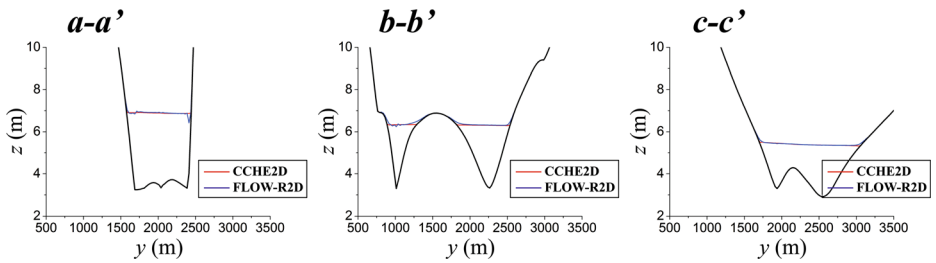

Fig. 9 Cross-sections with CCHE2D and FLOW-R2D models for T=50 years at x=2 km, x=4 km and x=6 km

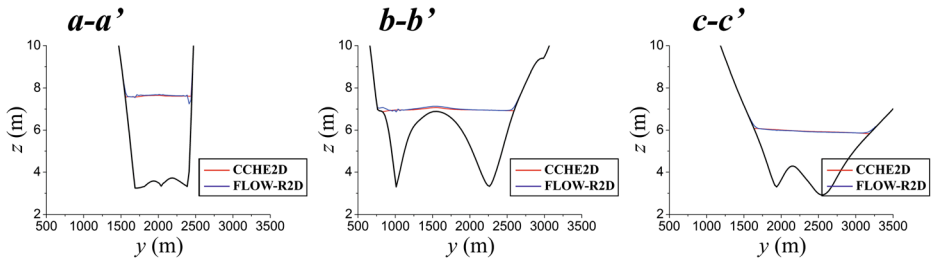

Fig. 10 Cross-sections with CCHE2D and FLOW-R2D models for T=500 years at x=2 km, x=4 km and x=6 km

In both scenarios and for both models, downstream boundary conditions are determined as open boundaries (kinematic wave) and there was no determination of lateral boundary conditions. The threshold of dry bed was determined $h_{dry}=3\times10^{-2}$ m in both models. As far as the time step is concerned, in FLOW-R2D model, Courant number is determined CFL=0.2 and in CCHE2D model, time step is steady Δt=0.1 s. Finally the diffusion factor in FLOW-R2D model is determined ω=0.9. The terrain data are exported from GIS maps with each cell being 25×25 m and therefore the space step in both directions was taken equal to 25 m. The computational grid comprises 247×401 cells.

Apart from the graphical comparison, the correlation indicators which were presented previously are also calculated in order to examine the correlation between the results of the two models. In Table 2, the respective indicators for water depths and water velocities are presented. As it is shown from the graphical comparison and from statistical indicators, the comparison between results of the two models is quite satisfactory.

It should be mentioned that the steady discharge as an upstream boundary condition is determined in a different way in the two models. Therefore, there are differences in the results of the two models in the upstream sections of the computational field which can be attributed partly to this item. There are also problems with CCHE2D model related to the downstream boundary conditions (there is no flow permanent situation with open boundary conditions in the downstream section). As far as the computational cost is concerned, it should be mentioned that FLOW-R2D achieved the solution of these scenarios 5–6 times faster.

One of the main objectives for developing FLOW-R2D model is the production of flood hazard maps as described by the Flood Directive 2007/60 of the EU. In the following figures, the flood hazard maps are presented for T=500 years scenario,

Table 2 Indicators for the comparison of the results of water depths and water velocities between FLOW-R2D and CCHE2D models

Return period	T=50 years				T=500 years			
Time	t=1 h		t=3 h		t=1 h		t=2 h	
Variable	h	V	h	V	h	V	h	V
PCC	0.97	0.88	0.95	0.88	0.98	0.90	0.98	0.91
NSE	0.94	0.75	0.87	0.77	0.95	0.80	0.95	0.82
IA	0.98	0.94	0.97	0.94	0.99	0.95	0.99	0.95

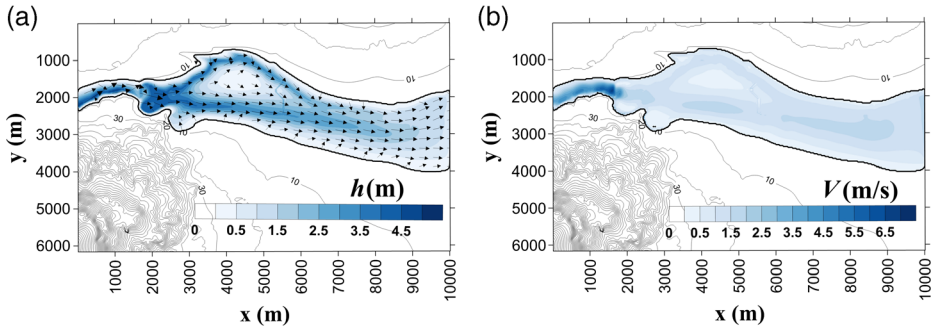

Fig. 11 **a** Water depths for T=500 years scenario in permanent situation with FLOW-R2D model **b** Water velocities for T=500 years scenario in permanent situation with FLOW-R2D model

which consist of water depth and water velocity in the entire computational field (Fig. 11a-b).

7 Conclusion

A new fully hydrodynamic model for flood routing in mild terrain areas was presented and tested. The model is based on the solution of 2D Shallow Water Equations using the Finite Difference Method through the explicit McCormack numerical scheme. The model is capable of incorporating detailed digital terrain data and of capturing shocks in complex terrains which often occur in built-up environments.

The model is tested using analytical and experimental data as well as results from another powerful model, extensively tested in the past, the CCHE2D model, which is based on a different methodological approach.

The modification of the McCormack numerical scheme with the introduction of artificial viscosity through a diffusion factor adopted in this study, seems to improve the validity of the model. Also, the adopted numerical technique which distinguishes wet/dry cells of the computational domain by means of a threshold can simulate the flood wave along a completely dry bed (e.g. urban environment or the downstream area of a dam). Combining low values of this threshold with the successful representation of the solid wall boundaries, FLOW-R2D model becomes a powerful model for simulating floods in built-up areas, in which very shallow flows are dominant. The model is also capable for producing detailed simulation of flood routing in floodplains with complex terrain.

Acknowledgments Acknowledgements are expressed to Dr S. Frazao for the provision of the experimental data and to Mr N. Kitou (MSc) for his valuable suggestions during the development of the algorithm of FLOW-R2D model.

Appendix

Generally, the truncation error is determined by subtracting the results of the exact solution of a PDE from the results of the finite difference solution. In our case (2D-SWE through McCormack numerical scheme), the exact solution is represented by Eq. 1 and the numerical solution by Eqs. 4 and 5.

In order to calculate the additional truncation error which was due to the modification of McCormack numerical scheme, the added quantity in corrector step of the numerical method should be determined. Specifically, this quantity is in Eq. A1:

$$\frac{1-\omega}{2}W_{i,j}^{k}+\frac{1-\omega}{8}\left(W_{i+1,j}^{k}+W_{i-1,j}^{k}+W_{i,j+1}^{k}+W_{i,j-1}^{k}\right) \tag{A1}$$

Through Taylor expansion series, the terms which are added become:

$$W_{i+1,j}^{k}=W_{i,j}^{k}+\Delta x\frac{\partial W}{\partial x}+\Delta x^{2}\frac{\partial^{2}W}{\partial x^{2}}+\ldots \tag{A2}$$

$$W_{i-1,j}^{k}=W_{i,j}^{k}-\Delta x\frac{\partial W}{\partial x}+\Delta x^{2}\frac{\partial^{2}W}{\partial x^{2}}+\ldots \tag{A3}$$

$$W_{i,j+1}^{k}=W_{i,j}^{k}+\Delta y\frac{\partial W}{\partial y}+\Delta x^{2}\frac{\partial^{2}W}{\partial y^{2}}+\ldots \tag{A4}$$

$$W_{i,j-1}^{k}=W_{i,j}^{k}-\Delta y\frac{\partial W}{\partial y}+\Delta x^{2}\frac{\partial^{2}W}{\partial y^{2}}+\ldots \tag{A5}$$

If Eqs. A2–A5 are inserted in Eq. A1, the added quantity of Eq. A1 becomes:

$$\frac{(1-\omega)}{4}\Delta x^{2}\frac{\partial^{2}W}{\partial x^{2}}+\frac{(1-\omega)}{4}\Delta y^{2}\frac{\partial^{2}W}{\partial y^{2}}+\ldots \tag{A6}$$

The above expression consists of the truncation error (TE_{ω}) associated to the second derivative which adds artificially diffusion terms in the classical form of McCormack numerical scheme and simultaneously does not change the order of accuracy. These diffusion terms seem to be appropriate in order to smooth out the oscillations which are produced by dispersion errors, especially during the simulation of flood wave propagation in complex topography, where these errors in most of the cases create instabilities in the numerical model. These artificially inserted diffusion terms can also describe the diffusion which is produced due to viscosity of the water and hence they are called artificial viscosity.

References

Abbott MB (1979) Computational hydraulics. Pitman Publishing Ltd., UK

Anastasiou K, Chan CT (1997) Solution of the 2D shallow water equations using the finite volume method on unstructured triangular mesh. Int J Numer Methods Fluids 24:1225–1245

Bellos V (2012) Ways for flood hazard mapping in urbanised environments: a short literature review. Water Utility Journal 4:25–31

Chaudhry MH (2008) Open channel flow, 2nd edn. Springer Editions, New York

Emelen VS, Soares-Frazao S, Riahi-Nezhad KC, Chaudhry MH, Imra J, Zech Y (2012) Simulations of the New Orleans 17th street canal breach flood. J Hydraul Res 50(1):70–81

Erpicum S, Dewals BJ, Archambeau P, Pirotton M (2010) Dam break flow computation based on efficient flux vector splitting. J Comput Appl Math 234:2143–2151

European Parliament, Council (2007) Directive 2007/60/EC of the European Parliament and of the Council of 23 October 2007 on the assessment and management of flood risks (Text with EEA relevance). OJ L 288:27–34

Fiedler FR, Ramirez JA (2000) A numerical method for simulating discontinuous shallow flow over an infiltrating surface. Int J Numer Methods Fluids 32:219–240

Guangcai S, Wenli W, Liu YL (2010) Numerical scheme for simulation of 2D flood waves. Proceedings of the International Conference on Computational and Information Science, Chengdu. pp 846–849

Gwo-Fong L, Jihn-Sung L, Wen-Dar G (2003) Finite volume component-wise TVD schemes for 2D shallow water equations. Adv Water Resour 26:861–873

Hunter NM, Bates PD, Néelz S, Pender G, Villanueva NG, Wright NG, Liang D, Falconer RA, Lin B, Waller S, Crossley AJ, Mason DC (2008) Benchmarking 2D hydraulic models for urban flooding. Water Manag 161(1):13–30

Jia Y, Wang SSY (1999) Numerical model for channel flow and morphological change studies. J Hydraul Eng 125(9):924–933

Katopodes ND, Strelkoff T (1979) Two-dimensional shallow water-wave models. J Eng Mech Div ASCE 105(4):317–334

Koutsoyiannis D, Mamasis N, Efstratiadis A (2003) Hydrological study of Sperhios river basin. Report on: 'Hydrological and hydraulic study for the flood protection of the new double railway line passing through Sperhios river basin', ERGA OSE S.A. (in greek)

Liang D, Lin B, Falconer RA (2006) Simulation of rapidly varying flow using an efficient TVD-McCormack scheme. Int J Numer Methods Fluids 53:811–826

Liang D, Lin B, Falconer RA (2007) A boundary-fitted numerical model for flow routing with shock-capturing capability. J Hydrol 332:477–486

McCormack RW (1969) The effect of viscosity in hypervelocity impact cratering. AIAA Hypervelocity Impact Conference, Cincinnati. Paper 69–354

Nash JE, Sutcliffe JV (1970) River flow forecasting through conceptual models, part I - a discussion of principles. J Hydrol 10(3):282–290

Néelz S, Pender G (2009) Desktop review of 2D hydraulic modelling packages. Environmental Agency, Bristol

Parker DJ, Priest SJ (2012) The fallibility of flood warning chains: can Europe's flood warnings be effective? Water Resour Manag 26:2927–2950

Pearson K (1895) Note on regression and inheritance in the case of two parents. R Soc Proc 58:240–242

Soares-Frazao S (2007) Experiments of dam-break wave over a triangular bottom sill. J Hydraul Res 45(Extra Issue):19–26

Testa G, Zuccalà D, Alcrudo F, Mulet J, Soares-Frazao S (2007) Flash flood flow experiment in a simplified urban district. J Hydraul Res 45(Extra Issue):37–44

Tsakiris G (2013) Flood risk assessment: concepts, modelling, applications. Nat Hazards Earth Syst Sci 2(1): 261–286

Tsakiris G, Nalbantis I, Pistrika A (2009) Critical technical issues on the EU flood directive. Eur Water 25(26): 39–51

Vreugdenhil CB (1994) Numerical methods for shallow-water flow. Water science and technology library, 13. Kluwer Academic Publishers, The Netherlands

Willmott CJ (1981) On the validation of models. Phys Geogr 2:184–194